Mesoporous silica nanoparticle-based protein delivery systems for biomedical applications

Tu, J.

Chapter IV

Membrane Fusion Mediated Intracellular Delivery of Lipid Bilayer Coated Mesoporous Silica Nanoparticles

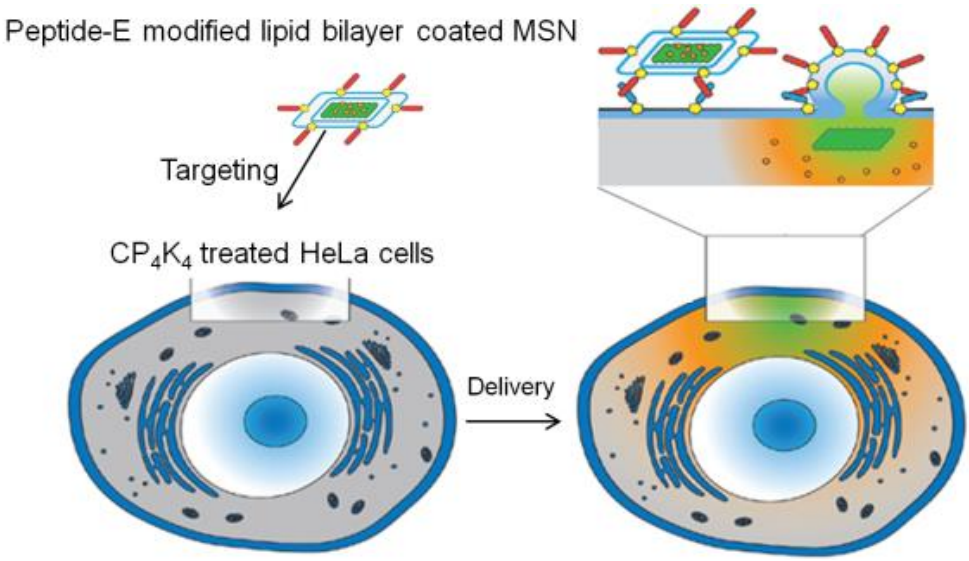

Jing Tu, Jian Yang, Gerda E. M. Lamers, René C. L. Olsthoorn and Alexander Kros

Abstract

Protein delivery into the cytosol of cells is a challenging topic in the field of nanomedicine, because cellular uptake and endosomal escape are typically inefficient, hampering clinical applications. In this contribution cuboidal mesoporous silica nanoparticles (MSNs) containing disk-shaped cavities with a large average pore diameter (10 nm) were studied as a protein delivery vehicle. Cytochrome c (*cyt*. c) was used as a model membrane-impermeable protein and encapsulated into MSNs (MSNs/*cyt*. c) with fast kinetics and high loading efficiency. To enhance the colloidal stability and to prevent the premature release of *cyt*. c before cellular uptake, the protein loaded MSNs were coated with a fusogenic lipid bilayer. Cellular uptake was enhanced by a complementary pair of coiled-coil forming lipopeptides, which were incorporated into the lipid bilayer of the MSNs particles and the cytoplasmic membrane respectively. Coiled-coil induced membrane fusion led to cytosolic delivery of the *cyt*. c loaded MSNs. Cell uptake inhibition studies with five commonly used inhibitors revealed that indeed endocytosis is not the major pathway of uptake, strongly suggesting that membrane fusion is the dominant uptake mechanism. In contrast, when one of the coiled-coil peptides was omitted the major route of uptake was endocytosis. The release and bioactivity of *cyt*. c inside cells was quantified using a caspase assay. It showed that the cells were driven into apoptosis, confirming the cytosolic delivery. This system is suitable for delivery of any other protein or other high molecular weight compound due to the large pore size of the MSNs and combined with coiled-coil mediated delivery has many potential applications in the field of biomedicine and diagnostics.

Keywords: intracellular delivery, lipid bilayers, coiled-coil, apoptosis, nanomedicine, mesoporous silica nanoparticles

4.1 Introduction

Intracellular protein delivery holds enormous promise for a range of biomedical applications,[1] such as cancer therapy,[2,3] vaccination and enzyme based therapeutics.[4] However, therapeutic proteins are susceptible to proteolysis and denaturation, limiting their efficacy in the body.[5,6] Thus, a variety of protein delivery systems have been developed in an attempt to solve the delivery problem, such as polymeric nanoparticles,[7] hydrogels,[8, 9] and lipid-based nanoparticles.[10, 11] Mesoporous silica nanoparticles (MSNs) have shown to be good carriers for a wide variety of biomolecules with varying molecular weight, including anticancer drugs, oligonucleotides and proteins.[2, 12-21] However, most MSNs used in drug delivery studies to date have typically pores with diameters up to 4 nm, thereby limiting their use as an efficient carrier for high molecular weight molecules like proteins. As a result, most studies show only low loading capacities and since the MSN pores are generally too small, offer weak proteolytic protection.[22]

Recently our lab developed sub-100nm MSNs with disk-like cavities that have large diameter pores (10 nm) able to encapsulate proteins with a wide molecular weight range and with high capacity and efficiency. While the use of MSNs as a drug delivery carrier has grown exponentially in the last decade, the long-term colloidal stability remains a challenge. Especially in *in vivo* experiments, it is critical that MSNs do not aggregate as this will negatively affect the bio-distribution and concomitant delivery of the drug. To enhance the colloidal stability lipid bilayer on the outer surface of MSNs have been introduced. This lipid bilayer coating also provides protection against enzymatic degradation,[23, 24] DNA break-down[25] and antibody neutralization,[26] resulting in prolonged retention of attached protein activity *in vivo* as long as the proteins remain immobilized within the MSNs carriers. Another advantage of lipid bilayer coated MSNs is the better control over the cargo release.[27, 28] For example, Roggers *et al*. showed that the controlled release of a model compound (fluorescein) was dependent on the removal of the lipid bilayer. In this case this was achieved by cleavage of the covalently bound lipids from dipalmitoylated MSNs.[29]

Lipid bilayers typically used to coat MSNs are composed of cationic lipids like DOTAP,[25, 30] neutral compounds like DPPC and cholesterol.[31] The pathway of cellular uptake of these lipid bilayer coated MSNs is via by endocytosis or macropinocytosis, which limits the delivery efficiency into the cytosol of cells. To the best of our knowledge, reports about the direct cytosolic delivery of MSNs do not exist yet.

Recently, we developed a new method to deliver anion transporters into the membrane of live cells based on membrane fusion of liposomes with cells.[32, 33] Here a complementary pair of coiled-coil lipopeptides was used to trigger fusion between liposomes and control targeted delivery.[34] These peptides, denoted E and K, were conjugated to cholesterol *via* a small polyethylene glycol (PEG) spacer, resulting in CPE and CPK.[35-38] When these lipopeptides were embedded in the lipid bilayer of liposomes and/or cell membranes respectively, triggered membrane fusion with concomitant release of liposome encapsulated cargo was observed.[39, 40]

To date, only liposomes with an aqueous core loaded with low molecular weight water soluble drugs, anticancer drugs or hydrophobic ion transporters located in the lipid bilayer of liposomes were fused with live cells.[32] More recently liposomes containing the anticancer drug doxorubicin could target modified HeLa cancer cells in a zebrafish xerograft model, resulting in targeted cell death.[41] Here, we would like to study whether coiled-coil lipopeptide mediated membrane fusion could be used to enhance the delivery of protein loaded MSNs into cells and to circumvent the endocytic pathway (Figure 4.1a). Cytochrome c (*cyt*. c) was chosen as a model protein as its cytosolic delivery activates the intrinsic apoptotic pathway. This allowed us to monitor the efficient uptake and delivery of *cyt.* c loaded MSNs as well as the induction of apoptosis[42] by cytosolic release of *cyt.* c.

4.2 Materials and Methods

4.2.1 Materials

Cytochrome c from equine heart, pluronic P123 ($EO_{20}PO_{70}EO_{20}$), tetraethyl orthosilicate (TEOS), HOBT, mesitylene, cholesterol (CHO) and Atto 488 NHS ester were purchased from Sigma-Aldrich and used as received. 1,2-dioleoyl-sn-glycero-3-phosphocholine (DOPC), 1,2-dioleoyl-sn-glycero-3-phosphoethanolamine (DOPE) and 1,2-dioleoyl-sn-glycero-3-phosphoethanolamine-N-(7-nitro-2-1,3-benzoxadiazol-4-yl) (ammonium salt) (DOPE-NBD) were purchased from Avanti Polar Lipids. Fmoc-protected amino acids were purchased from Novabiochem. All other reagents and solvents were obtained at the highest purity available from BioSolve or Sigma-Aldrich and used without further purification. 8-wells slide Lab-tek was purchased from Thermo Scientific. DMEM medium was obtained from Gibco. WST-1 was obtained from Serva. PMS-Ome was obtained from Santa Cruz Biotechnology. Apo-ONE® Homogeneous Caspase-3/7 Assay kit was purchased from Promega. The composition of PBS was K_2HPO_4 (14.99 mM), KH_2PO_4 (5 mM), and NaCl (150.07 mM) and PB was composed of Na_2HPO_4 (1 mM) and NaH_2PO_4 (1 mM) at a molar ratio of 5:2. The pH was 7.4.

4.2.2 Characterization of MSNs and LB-MSNs

TEM images were collected by using a JEOL 1010 instrument with an accelerating voltage of 70 kV. Nitrogen adsorption-desorption isotherms were obtained with a Micromeritics TriStar II 3020 surface area analyzer. Before each measurement, MSNs were outgassed in the vacuum (below 0.15 mbar) at 300 °C for 16 h. The specific surface areas were calculated from the adsorption data in the low pressure range using the Brunauer-Emmett-Teller (BET) model.[43] The pore size distribution was determined following the Barrett-Joyner-Halenda (BJH) model.[44] The hydrodynamic size distribution and zeta-potential of the samples were measured with a Malvern Nano-zs instrument.

4.2.3 Synthesis of lipopeptides

Peptides E_4 $(EIAALEK)_4$ and K_4 $(KIAALKE)_4$ were synthesized on a 250 µmol scale using Fmoc chemistry on a CEM peptide synthesizer. Sieber amide resin with a loading of 0.69 mmol/g was used. Amino acid couplings were performed with 4 eq. of the appropriate amino acid, 4 eq. of the activator HCTU and 8 eq. of the base DIPEA. Fmoc deprotection was performed with piperidine:NMP (4:6 v/v). N_3-PEG_4-COOH[36] was coupled to the N-terminus of the peptide using 4 eq. of DIPEA and 3 eq. of HOBT in DMF for 18 hours. The azido group was reduced to NH_2 using 8 eq. of trimethylphosphine (1 M in toluene) in a dioxane/H_2O mixture (4:1 v/v) for 2 h reaction, this reaction was performed twice. In the final step cholesteryl-4-amino-4-oxobutanoic acid (2 eq.) was coupled to the PEG_4 linker using 5 eq. of DIPEA and 4 eq. of PyBOP in DMF for 72 h. The resulting lipopeptides CP_4K_4 and CP_4E_4 were cleaved from the resin with a mixture of TFA/TIS/H_2O (95:2.5:2.5 v/v) for 1.5 h. The cleavage mixture was precipitated in cold diethyl ether. The precipitate was collected and the crude product was purified by HPLC using a C4 column.[40]

4.2.4 Synthesis of large pore MSNs

0.5 g of surfactant Pluronic P123 and 1.4 g of FC-4 were dissolved in 80 ml of HCl (0.02 M), followed by the addition of 0.48 ml of TMB.[45] After stirring for 6 h, 2.14 ml of TEOS was added dropwise. The resulting mixture was stirred at 30 °C for 24 h and transferred to an autoclave at 120 °C for 2 days. Finally, the solid product was isolated by centrifugation (13000 rpm, 5 min), washed with ethanol and water. The organic template was completely removed by calcination at 550 °C for 5 h in air.

4.2.5 Labeling of cytochrome c with Atto 488 NHS Ester

Cytochrome c (10 mg) was dissolved in 5 ml of sodium carbonate buffer (100 mM, pH 8). Atto 488 NHS ester was dissolved in DMSO (2 mg/ml), and 0.5 ml of this solution was added to the protein solution. The mixture was stirred for 4 h at room temperature. The resulting Atto 488-labeled protein was purified by size exclusion chromatography using a Sephadex-G25 column, PBS as eluent.

4.2.6 Liposome preparation

Stock solutions of phospholipids (1 mM) in $CHCl_3$ and CP_4E_4 (50 μM) in $CHCl_3$:CH_3OH (1:1) were prepared and stored at −20 °C. The stock solutions were mixed to obtain the desired liposome formulation (DOPC: DOPE: CHO = 2:1:1 molar ratio). Liposomes were prepared by mixing the appropriate amount of lipids and CP_4E_4 in a 20 mL glass vial and evaporating the solvents to form a lipid film. The film was rehydrated with 1 ml of phosphate buffer (1 mM PB, pH 7.4). The solution was vortexed for 30 seconds to form a cloudy lipid suspension and sonicated in a water bath at 50 °C for 10 min. The resulting liposomes were stored at 4 °C (final lipid concentration was 1 mM) and the hydrodynamic diameter as determined by DLS was approximately 100 nm. The final concentration of lipids and CP_4E_4 in each sample used in the cell experiments was 250 μM and 2.5 μM, respectively.

4.2.7 CP_4K_4 solution

A CP_4K_4 stock solution (100 μM) was prepared in $CHCl_3$: CH_3OH (1:1). An appropriate amount of CP_4K_4 stock solution was added in a glass vial and the organic solvent was evaporated under a N_2 flow. The obtained film was hydrated and diluted by DMEM (+/- FCS, w/o phenol red) and sonicated at 55 °C for 1 min. The final concentration of CP_4K_4 was 5 μM.

4.2.8 Loading Cyt. c into MSNs

Cytochrome *c (cyt. c)* solutions with various concentrations (0.25, 0.5, 1, 2 and 4 mg/ml) were prepared in phosphate buffer (1 mM, pH 7.4). MSNs (2 mg/ml) were dispersed in the same buffer by sonication (10 min). In a typical procedure, 0.5 ml of *cyt.* c stock solution was mixed with 0.5 ml of MSNs and incubated and shaken with an Eppendorf ThermoMixer for 5 min (400 rpm, 25 °C). The *cyt.* c-loaded MSNs were collected by centrifugation (10000 rpm, 5 min) and separated from non-encapsulated *cyt.* c, which remained in the supernatant. The pellet was resuspended in 1 ml of PB (1 mM, pH 7.4) and the zeta-potential was measured. The absorbance of non-encapsulated *cyt.* c was measured in the supernatant using Greiner 96-

well flat-bottom transparent in a plate reader (Tecan infinite M1000). A calibration curve was determined based on the absorbance at 412 nm[46] as a function of *cyt.* c concentration (0-500 µg/ml).

4.2.9 Preparation of MSNs/cyt. c@CPE-LBs

A solution of MSNs/*cyt.* c (1 mg/ml; 0.5 ml) was transferred into 1 ml of freshly prepared CPE liposomes (0.5 ml; [lipid]= 0.1 mM containing 1 mol% CP_4E_4) and the mixture was shaken with a Eppendorf ThermoMixer (25 °C, 400 rpm) for 90 min. And subsequently centrifuged at 10000 rpm for 3 min. The supernatant was removed and the pellet was washed 3 times with 1 ml of PB and 3 times with DMEM (-FCS, -phenol red). The pellet was resuspended in DMEM at a final concentration of 1 mg/ml based on the MSNs' weight.

4.2.10 Cyt. c release profile from MSNs

The *in vitro* release of *cyt.* c from MSNs was determined at 37 °C. *Cyt.* c loaded MSNs with or without a lipid bilayer were suspended in 1 ml of pre-warmed PBS (pH 7.4) or PB (pH 7.4) respectively and incubated at 37 °C on an Eppendorf ThermoMixer (400 rpm). Supernatants were collected thoroughly by a pipette after centrifugation and 1 ml of fresh PBS were added at different time points. The released amount of *cyt.* c from MSNs at the different time points were quantified by measuring the absorption of the Soret band of *cyt.* c at 412 nm.[5] Each experiment was repeated three times.

4.2.11 Cell culture

HeLa cells were grown as a monolayer at 37 °C in 7% CO_2 atmosphere, and were maintained in a continuous logarithmic culture in Dulbecco's Modified Eagle Medium (DMEM) containing phenol red completed with 10% Fetal Calf Serum (FCS), penicillin/ streptomycin (100 units/ml, 0.1 mg/ml, respectively), and Glutamax (2 mM). The medium was replaced every 3 days and cells were passaged by trypsinization at 70% confluence.

4.2.12 Cell viability assay

Cells were seeded in a 96 well-plate at a concentration of 1×10^4 cells per well and incubated for 24 h prior to the WST-1 assay. The medium was removed and cells were incubated with 100 µL of a CP_4K_4 (5 µM) solution in medium (w/o phenol red) for 2 h. The medium containing CP_4K_4 was removed after 2 h and the cells were washed three times with 250 µl of DMEM medium. Next the cells were incubated with 250 µl (1 mM total lipid) lipid

coated MSNs containing 1 mol% CP_4E_4 for 1 h. Next, the lipid coated MSNs were removed and fresh medium was added to each well and the plate was incubated at 37 °C to perform a WST-1 assay.[47] The medium containing WST reagent was removed after 24 h and 200 µl of cell proliferation reagent WST-1 in DMEM (w/o phenol red) was added to each well and the cells were incubated for 3 h at 37 °C. Absorption was measured (at 450 nm) at room temperature using a Tecan Infinite M1000 PRO microplate reader, the cells were shaken for 60 s prior to each measurement (2 mm linearly, 654 rpm). The Z-position was 12500 µm, and the gain was optimized according to the amount of fluorophore in the sample. The metabolic activity (cell survival) were normalized with respect to the control (*i.e.* non-treated cells), which was set to 100%. For the control experiments, cells were incubated with MSNs@CPE-LB, only MSNs or MSNs@LB in the absence of lipopeptides.

4.2.13 Transmission electron microscopy (TEM)

1×10^6 HeLa cells per well were seeded on 15 mm thermanox coverslips and fixed with 2 v% glutaraldehyde in a sodium cacodylate buffer (0.1 M, pH 7.2) for 2 h at room temperature. Post fixation was performed with 1% w/v osmium tetroxide in distilled water for 1 h at room temperature. The cells were dehydrated through a graded series of ethanol and embedded in Agar 100 resin (Agar Scientific, AGR1043) and the sections where cut with a diamond knife at a Leica Ultramicrotome. Microscopy images were obtained with a JEOL JEM-1010 transmission electron microscope with a maximum output voltage up to 80 KV (Tokyo, Japan) equipped with an Olympus Megaview camera (Tokyo, Japan).

4.2.14 Confocal imaging

Cells were grown in an 8-well slide at a density of 2.5×10^4 cells per well and incubated in the DMEM (+FCS, -phenol red) at 37 °C under a 7% CO_2 atmosphere. The medium was removed after 21 h and a CP_4K_4 solution (5 µM, 300 µl) was added and incubated for 0.5-2 h at 37 °C under a 7% CO_2 atmosphere. The CP_4K_4 solution was removed and the cells were washed 3 times with 250 µl fresh DMEM (+FCS, -phenol red), and incubated with *cyt.* c or with CPE_4-decorated lipid bilayers coated MSNs loaded with *cyt.* c (250 µM, 300 µl). After 15 min of incubation, the cells were washed three times and fluorescent images were acquired on Nikon confocal laser scanning microscope. Nikon application suite advanced fluorescence software and Image-J was used for image analysis. The wavelength setting for Atto488 labeled *cyt.* c was Ex/Em: 501/523 nm (Ex laser: 480 nm), for Hoechst 33342 was Ex/Em: 361/497 nm (Ex laser: 420 nm).

4.2.15 Endocytosis inhibition measurements

HeLa cells were seeded in a 24-well plate at a density of 1×10^5 cells per well and incubated in DMEM (+10% FCS, -phenol red) medium at 37 °C. The medium was removed after 21 h and the cells were incubated with 500 µL of nocodazole (40 µM), wortmannin (0.25 µM), chlorpromazine (40 µM), genistein (200 µM), or sodium azide 0.01% w/v in DMEM (-FCS, -phenol red) medium. After 1 h of pre-incubation, the medium was removed and the cells were treated with 500 µl of CP_4K_4 (5 µM) supplemented with the above mentioned inhibitors for 2 h, after removed CP_4K_4 and washing 3 times with medium, followed by the addition of 100 µl of MSNs@CPE-LBs (the concentration of MSNs was 1 mg/ml). After 30 min, liposomes and inhibitors were removed and HeLa cells were washed 3 times by DMEM medium. The cells were incubated at 37 °C for 1 h. Next, the cells were detached using PBS/EDTA (10 mM EDTA) for 15 min, centrifuged and re-suspended in fresh medium at a concentration of 2×10^5 cells/ml. The mean fluorescence intensity of Atto 488 of the cells was measured by flow cytometry using a Beckman Coulter Quanta SC machine.

4.2.16 Apoptosis assay

HeLa cells at the density of 1×10^4 per well in 96-well plate were cultured in DMEM (+10% FCS, -phenol red) medium at 37 °C prior to the apoptosis assay. HeLa cells were treated a CP_4K_4 solution at the concentration of 5 µM for 2 h, following CP_4K_4 was removed, cells were washed 3 time with medium and incubated with MSNs/*cyt.* c@CPE-LB for 0.5 h. Next, the cells were washed with 100 µl medium 3 times and incubated at 37 °C with 7% CO_2 for 30 h or 48 h, finally, 100 µl of the Apo-ONE® Homogeneous Caspase-3/7 Assay reagent was added for each well and incubated for 3 h. The caspase activity was measured as a function of the created fluorescent rhodamine 110, which is released upon the cleavage of the non-fluorescent caspase substrate Z-DEVD-R110 (bis-(N-CBZL-aspartyl-L-glutamyl-L-valyl-L-aspartic acid amide) by caspase 3/7 activity.[48] Wavelength settings: Ex/Em: 490/520 nm. Measurements were performed as three independent experiments using Greiner 96-well flat-bottom transparent in a plate reader (Tecan infinite M1000). Statistical analysis was performed to calculate average values and standard deviations.

4.3 Results and discussion

We synthesized a new type of cuboidal MSNs featuring a cuboidal-like geometry using a mixture of block copolymers (Pluronic P123), a pore expander (1,3,5-trimethylbenzene, TMB) and fluorocarbons (FC-4) as the structure-directing template. The resulting particles possess an array of disk-shaped mesochannels along the short axis of the rectangular shaped (90 ± 20 nm by lengths, 43 ± 7 nm by widths) MSNs as shown in the transmission electron micrographs (TEM) (Figure 4.1b). The nitrogen adsorption-desorption isotherms of MSNs exhibited the characteristic type IV isotherms according to International Union of Pure and Applied Chemistry (IUPAC) classification[49] with a BET surface area of 506 m^2/g (Figure 4.1c). The pore size distribution was measured by the BJH method[50] and found to be 10 ± 1 nm for the majority of MSNs.

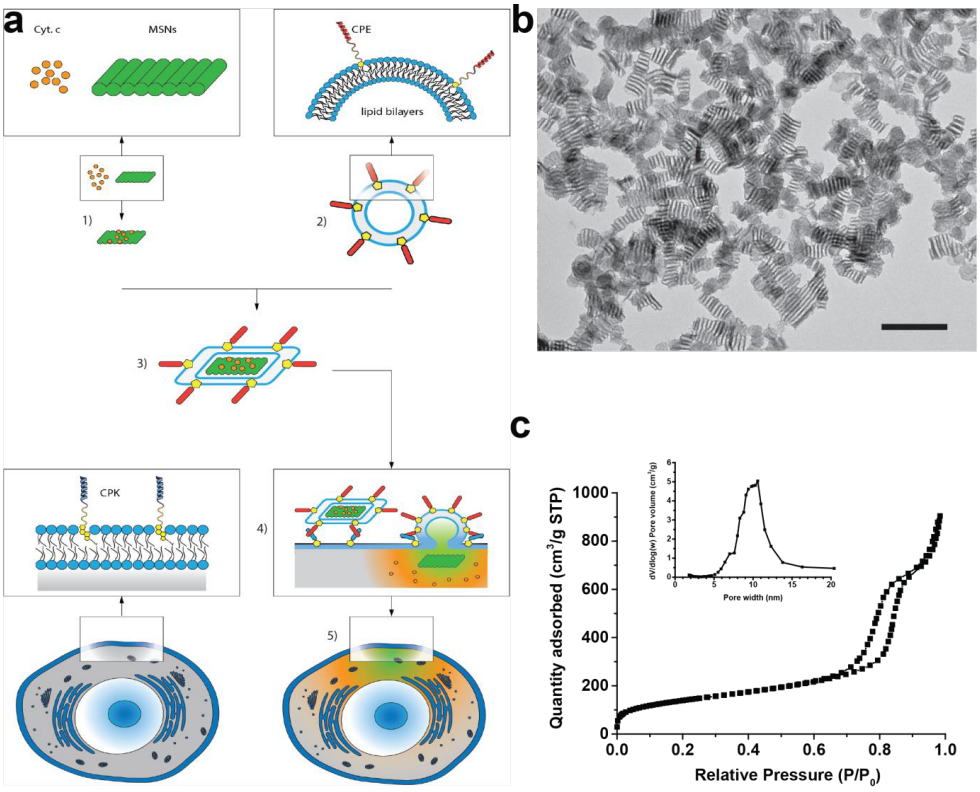

Figure 4.1 *Schematic illustrating the fusion between cells and lipid bilayer coated MSNs driven by coiled-coil formation between CP_4K_4 and CP_4E_4. (a) Intracellular delivery procedure 1) cyt. c (orange) is encapsulated into MSNs (green); 2) lipid bilayers (light blue) are decorated with lipopeptide CPE (red); 3) combining lipid bilayers (LBs) with MSNs/cyt.*

c; 4) incorporation of CP_4K_4 (dark blue) into cellular membrane and addition of CPE-coated MSNs trigger membrane fusion and delivery of cyt. c into the cytoplasm and 5) observation of cell membrane labeling and induction of cellular responses (e.g. apoptosis). (b) TEM image of MSNs, scale bar = 200 nm and (c) nitrogen adsorption-desorption isotherms and pore size distribution (insert).

We investigated whether this new type of MSNs could be used to transport proteins into the cytosol of cells. We chose to use cytochrome c (*cyt.* c, Mw 12384 Da, geometric size 2.6 × 3.2 × 3.3 nm) as a model protein. *Cyt. c* is a small redox protein that is present in the inner membrane of mitochondrion and induces apoptosis (programmed cell death) when it is released into the cytosol.[51] The pore dimensions of our cuboidal MSNs are sufficiently large to accommodate *cyt.* c. and the open disk-shaped mesostructure has a large surface area rendering the encapsulation of *cyt.* c very efficient. Dispersion of as-synthesized MSNs into a *cyt.* c stock solution resulted in a rapid adsorption of the protein inside the disk-like porous structure of the MSNs. The amount of absorbed protein was determined by measuring the difference in absorption of the Soret band (412 nm) in the supernatant before and after the encapsulation (Figure 4.2a).[46] Within 5 min an equilibrium in *cyt.* c adsorption was obtained and 95.49 ± 1.63% of *cyt.* c was encapsulated into the MSNs. The encapsulation capacity of MSNs was further investigated by incubating a fixed amount of MSNs (1 mg) with *cyt.* c at increasing concentrations (0.25-4 mg/ml). The maximum *cyt.* c loading capacity in these cuboidal MSNs was determined to be 470 μg/mg MSN (Figure 4.2a, black curve). The surface charge of *cyt.* c loaded MSNs as a function of initial *cyt.* c concentration was determined by measuring the zeta-potential (Figure 4.2a, red curve). When the protein concentration (0-1 mg/ml) was increased, the zeta-potential of MSNs/*cyt. c* tended to become neutral and remained around 0 mV at higher concentrations of *cyt. c* (1-4 mg/ml). When the weight ratio between *cyt.* c and MSNs was 1:8 or 1:4, the encapsulation efficiency (EE%) of *cyt.* c into MSNs was close to 100%, revealing the excellent protein encapsulation potential of this new type of cuboidal MSNs. As expected, the EE% decreased as the ratio of *cyt.* c/MSNs increased. Compared to native *cyt.* c, the encapsulated *cyt.* c in the MSNs revealed a slight broadening of the adsorption peak in the UV-Visible spectrum, but no blue shift was observed, suggesting that the interaction between the protein and pore surface did not change the structure of *cyt.* c.[52] The absorption maximum of the Soret band remained at 412 nm, showing that *cyt.* c retained its native fold and suffered no conformational change (Figure 4.S1a).[52, 53]

Next, the *in vitro cyt.* c release from MSNs was studied at 37 °C by measuring the Soret band (412 nm) of *cyt.* c in the supernatant as a function of time. The *cyt.* c adsorption is mainly driven by electrostatic interaction since *cyt.* c is positively charged at pH 7.4 while MSNs are negatively charged due to the silanol groups on the surface. [46, 54] Therefore, we studied the influence of ionic strength on the release profile. For this, MSNs/*cyt.* c were suspended in phosphate buffered saline (PBS, pH 7.4, ionic strength = 270 mM) and phosphate buffer (PB, pH 7.4, ionic strength = 12 mM), respectively. Next, the protein release as a function of ionic strength was determined over a period of 62 h (Figure 4.S1a). The amount of released *cyt.* c from MSNs was 70.4 ± 1.8% in PBS and only 16.8 ± 1.8% in 1 mM PB. At higher ionic strength of the buffer, the electrostatic interactions between *cyt.* c and MSNs are weakened resulting in an increased release of the protein. Thus *cyt*. c can be loaded with high efficiency into MSNs at low ionic strength and subsequently released at conditions of high ionic strength, confirming that the electrostatic interaction between *cyt.* c and MSNs contributed highly to the encapsulation and release process.

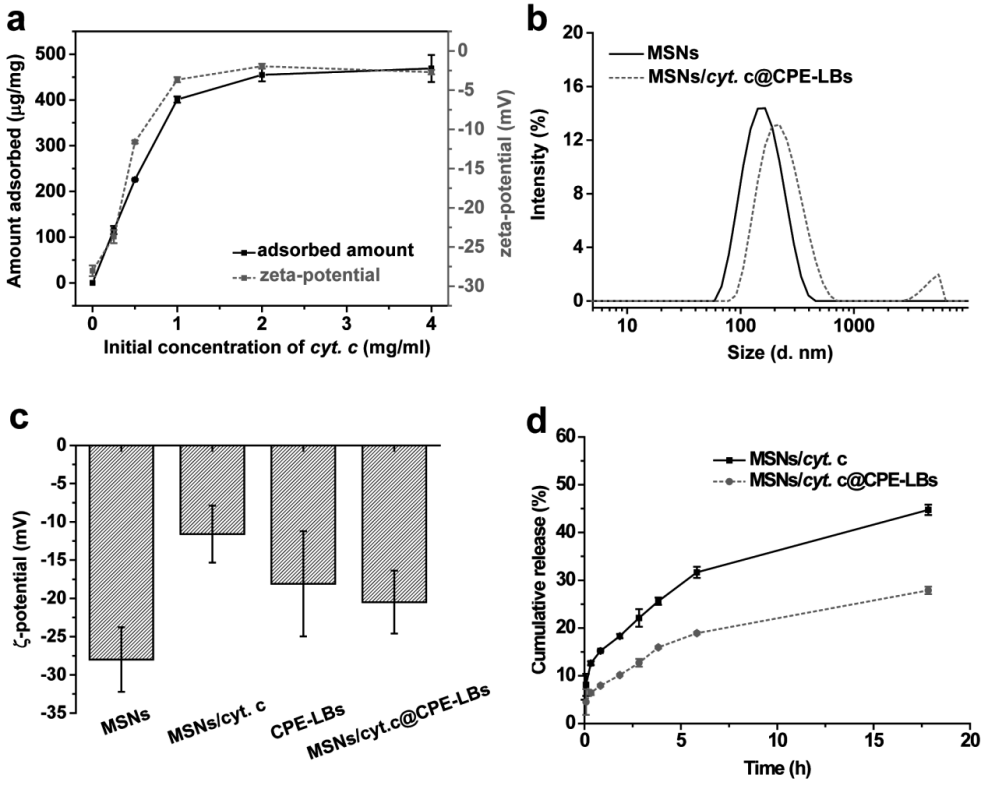

Figure 4.2 *Characterization of MSNs/cyt.* c *(a) Loading capacity and zeta (ζ)-potential of MSNs/cyt.* c*, with different initial cyt.* c *concentrations (0.5-4 mg/ml, 1 mM PB, pH 7.4.) (b)*

Dynamic light scattering (DLS) of MSNs and MSNs/cyt. c@CPE-LBs, 1 mM PB, pH 7.4. (c) Zeta-potential of MSNs, MSNs/cyt. c, CPE-LBs and MSNs/cyt. c@CPE-LBs (error bars represented zeta deviation, 1 mM PB, pH 7.4) and (d) in vitro release profiles of MSNs and MSNs/cyt. c@CPE-LBs in PBS, pH 7.4. Error bars show the standard deviation of three independent experiments.

The repulsive force between MSNs/*cyt.* c decreased when more protein was loaded into MSNs, as evidenced by the lower zeta-potential. As a result, MSNs/*cyt.* c tend to form aggregates more readily due to the decreasing surface charge. Indeed, dynamic light scattering (DLS) measurements revealed that after encapsulation, MSNs/*cyt.* c tended to aggregate as the hydrodynamic diameter increased to >2000 nm. In order to increase the colloidal stability, the MSNs/*cyt.* c were decorated with a lipid bilayer. After introduction of a lipid bilayer composed of DOPC, DOPE and Cholesterol (2:1:1 molar ratio,[35] the observed diameter by dynamic light scattering of the nanoparticles was reduced from ~2 μm to 229 nm (polydispersity index, PDI = 0.251) (Figure 4.2b). This lipid composition was chosen as it is known to be fusogenic when combined with the complementary lipopeptides CP_4E_4 and CP_4K_4.[40] After loading the MSNs with *cyt.* c, the zeta-potential shifted from -28.0 to -11.6 mV. Application of the lipid bilayer onto the exterior surface of these particles resulted in a more negative zeta potential (-20.5 mV) (Figure 4.2c). The presence of the lipid bilayer also reduced the burst release of *cyt.* c by a factor of ~1.6 fold as it acts as a barrier[55] retaining the protein more within the MSNs (Figure 4.2d).

Previously, we reported that the complementary coiled-coil lipopeptides $CP_{12}E_3$ and $CP_{12}K_3$ could be used to dock liposomes at the outer plasma membrane of live cells.[56] Extension of the lipopeptides with one heptad repeat of amino acids (*i.e.* CP_4E_4/CP_4K_4) resulted in membrane fusion between liposomes and cells using lipopeptides[32, 40] as evidenced by the delivery of low molecular weight dyes, anion transporter and the anticancer drug doxorubicin. To study the scope of this synthetic fusion system, we now were interested to study whether coiled-coil mediated fusion could be used to enhance the intracellular delivery of inorganic MSN. To date, MSNs or lipid bilayer coated MSNs are typically taken up by endocytosis,[14, 29, 55, 57, 58] which can be detrimental to the cargo. By employing coiled-coil mediated delivery using CP_4E_4 and CP_4K_4, the cellular uptake mechanism might be shifted from endocytosis to a direct cytosolic entry *via* membrane fusion. In order to enhance the intracellular delivery of MSNs/*cyt.* c, a fusogenic lipid bilayer composed of CP_4E_4 was therefore applied. In order to induce fusion, cells were pretreated with CP_4K_4. Next a

suspension containing CP_4E_4-lipid bilayer coated MSNs/*cyt.* c was added to the cells and incubated for 30 min. A cell viability assay demonstrated that CP_4E_4 / CP_4K_4, lipid bilayer coated MSNs with or without CP_4K_4 are well tolerated by HeLa cells after a 24 h post-treatment (Figure 4.S2). Confocal microscopy imaging revealed that the cytosol became fluorescent, indicative of the efficient delivery of Atto488-labeled *cyt.* c inside the cytosol (Figure 4.3a). In contrast, when one or both of the lipopeptides were omitted, and thus coiled-coil mediated fusion cannot occur, only a very limited cellular uptake of *cyt.* c was observed (Figure 4.S3). Furthermore, the incubation of cells with Atto488-labeled *cyt.* c alone did not result in any cellular uptake, revealing that the water-soluble protein cannot enter the cell by transient membrane destabilization or endocytosis. In contrast, by applying the coiled-coil mediated fusion system, *cyt.* c could be efficiently delivered to the cytosolic within 30 min.

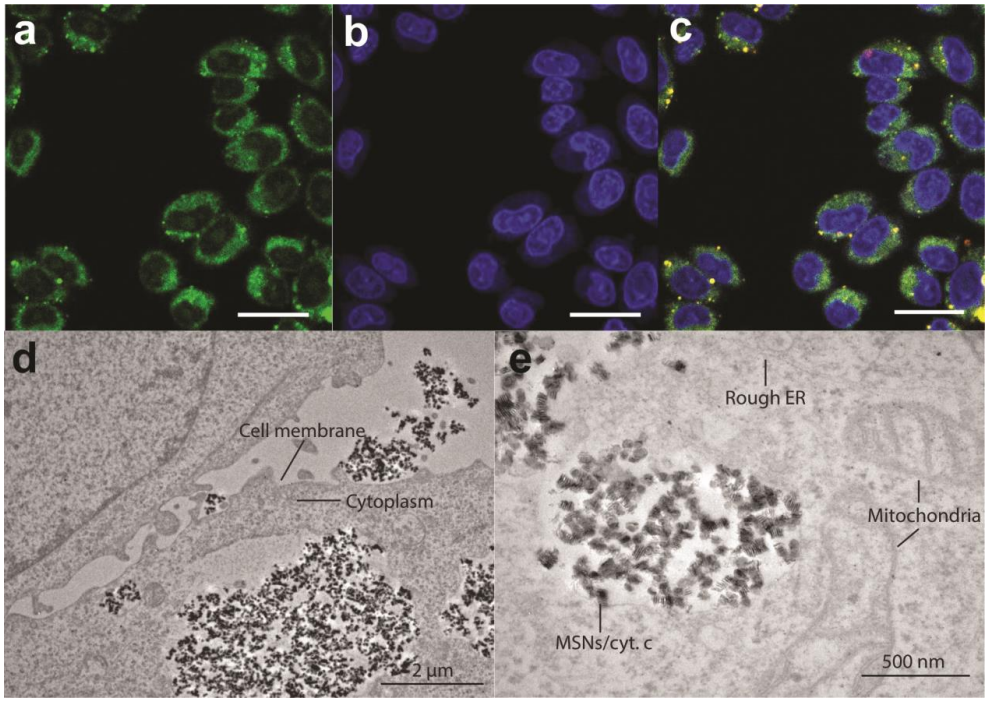

Figure 4.3 *Intracellular delivery of cyt. c by MSNs@CPE-LBs. (a-c) Confocal images showing: (a) location of Atto488 labeled cyt. c, (b) cell nuclei stained by Hoechst and (c) overlay, scale bar = 25 µm. TEM images of (d) delivered MSNs/cyt. c@CPE-LBs into CP_4K_4 pretreated HeLa cells. Scale bar = 2 µm, (e) magnification showing details of cell organelles' structures, such as rough ER and mitochondria, scale bar = 500 nm.*

To obtain more details on the intracellular location of the MSNs upon CP_4K_4 / CP_4E_4 mediated delivery, we sectioned the cells. TEM imaging revealed the different stages of the intracellular uptake processes in HeLa cells. A fraction of the MSNs was still outside of the cell, some were entering into the cytoplasm and others had already entered the cytosol (Figure 4.3d). The MSNs were located close to mitochondria and rough ER and seemed to be aggregated (Figure 4.3e). A possible explanation might be that upon the delivery into the cells, the MSNs lose their lipid bilayers and bare MSNs are known for their tendency to aggregate. Strikingly, no membrane was observed around the aggregated MSNs, suggesting that the nanoparticles were not captured in endosomes or lysosomes. In comparison, the cell uptake efficiency of bare MSNs is relatively low (Figure 4.S3c). More importantly, in the control experiment the MSNs were located in early endosomal compartments as evidenced by the presence of a membrane bilayer (Figure 4.S4). These results show that coiled-coil driven membrane fusion enhances the cellular uptake.[14]

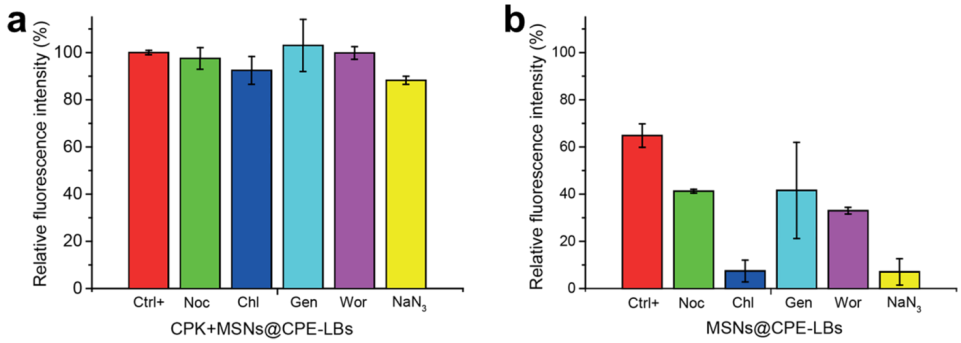

Figure 4.4 *Mechanistic cellular uptake study. Intracellular uptake of a lipid bilayer coated MSNs in the presence of endocytosis/micropinocytosis inhibitors. (a) Coiled-coil mediated cellular uptake of cyt. c and (b) control experiment in which CP_4K_4 was omitted, only MSNs@CPE-LBs were tested with endocytosis and micropinocytosis inhibitors. Ctrl+ = HeLa cells incubated with PBS; Noc = Nocodazole; Chl = Chlorpromazine; Gen = Genistein; Wor =Wortmannin; NaN_3 = Sodium azide. Error bars show the standard deviation of three independent experiments.*

To gain insight in the cellular uptake pathways, we repeated the lipid bilayer coated MSNs delivery in the presence of several well-known inhibitors using flow cytometry measurements (FACS) and confocal microscopy imaging. In this study, wortmannin was used as a micropinocytosis inhibitor as it blocks PI3-kinase[59-62] while genistein inhibits tyrosine-

phosphorylation of Cav 1 and caveolin-dependent endocytosis.[63-65] Furthermore, chlorpromazine was used as it blocks clathrin-dependent endocytosis,[66-68] and microtubule formation was inhibited by nocodazole. Uptake studies in the presence of these inhibitors will yield information on the intracellular trafficking and internalization mechanisms involved in the uptake of the lipid bilayer coated MSNs.[61, 62, 68-70] Finally, as endocytosis of nanoparticles is an energy-dependent process, sodium azide was used to deplete the energy demands for endocytosis and thus restrict metabolic activity.[71, 72]

HeLa cells were pre-incubated for 1 h with the above-mentioned inhibitors. After removal of the medium, the cells were treated with CP_4K_4 (5 μM) for 2 h and subsequently MSNs@CPE-LBs were added in the presence of freshly added inhibitors in the medium. FACS analysis revealed that genistein, wortmannin and nocodazole had no adverse effect on the delivery of fluorescently labeled *cyt.* c (Figure 4.4a), whereas in the presence of chlorpromazine and sodium azide, uptake of nanoparticles containing *cyt.* c was slightly lowered to 90% as compared to *cyt.* c uptake in the absence of inhibitors. To further study the role of coiled-coil formation in the mechanism of cellular uptake, we omitted the CP_4K_4 pretreatment of HeLa cells in a control experiment and added the MSNs/*cyt.*c@CPE-LBs directly to the cells. In the absence of inhibitors, the *cyt.* c uptake was already lowered to 60%, revealing the importance of coiled-coils for the efficient cellular uptake of the nanoparticles. In the presence of chlorpromazine and sodium azide, the uptake was sharply reduced to 10% (Figure 4.4b), which is in strong contrast with the previous experiments when CP_4K_4 was present, enabling coiled-coil mediated uptake (Figure 4.4a). This indicates that the nanoparticles are most likely taken up by a clathrin-dependent endocytosis pathway in the control experiment. Combining these inhibition studies indicated the dominant pathway for coiled-coil mediated MSNs delivery is most likely via membrane fusion between lipid bilayer coated MSNs and the cell membrane. In contrast, when coiled-coil formation cannot occur, the dominant but less efficient route of cellular uptake is via endocytosis.

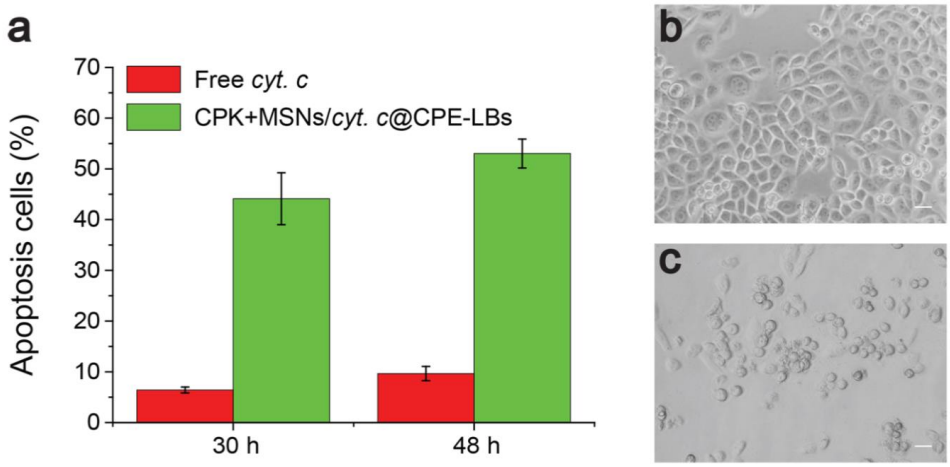

Figure 4.5 *Cytoplasmic cyt. c delivery induces apoptosis. (a) Percentage of apoptotic cells as measured by caspase activity, after 30 h and 48 h. Image of HeLa cells treated with (b) cyt.* c *and (c) MSNs/cyt. c@CPE-LBs where coiled-coil formation. HeLa cells were incubated with* CP_4K_4 *for 1 h, then with MSNs/cyt. c@CPE-LBs for 0.5 h. Caspase activity was determined after 30 h and 48 h. Error bars are standard deviation of three independent experiments. Scale bar =25 µm.*

It is well-known *cyt.* c in the cytosol triggers caspase activation,[73-75] which ultimately results in apoptosis of the cell.[51, 76] Coiled-coil mediated delivery and bioactivity of *cyt.* c via MSNs/cyt. c@CPE-LBs resulted in 60% of apoptosis after 48 h (Figure 4.5a), while free *cyt.* c induced only minor apoptosis (10%). The morphological changes of apoptotic HeLa cells versus healthy cells upon *cyt.* c delivery were evident (Figure 4.5b,c). In control experiments where one or both of the lipopeptides were omitted only minimal levels of apoptosis (< 10%) were observed, revealing that coiled-coil mediated delivery of MSNs@LBs is more efficient when compared to delivery via endocytic pathways (Figure 4.S5).

4.4 Conclusion

In conclusion we have developed MSNs with a high loading capacity for *cyt.* c due to their large disc-shaped cavities. The introduction of a lipid bilayer at the MSNs outer surface improved the colloidal stability and lowered the initial burst release of *cyt.* c. The cellular uptake of the MSNs resulting in cytosolic delivery of *cyt.* c was significantly enhanced by coiled-coil mediated membrane fusion. As a result, direct cytosolic delivery of *cyt.* c was

achieved while uptake via endocytosis was minimized. The uptake pathway and localization of MSNs/*cyt.* c in HeLa cells were confirmed by TEM and confocal imaging, and release of functional *cyt.* c was demonstrated by its ability to trigger apoptosis. We believe that our coiled-coil based system is suitable for delivery of other proteins or high molecular weight compounds due to the large pore size of the MSNs. This method will also enable the delivery of any other (in)organic nanoparticles as long as it can be encapsulated in a fusogenic lipid bilayer. Therefore it may have applications in the field of biomedicine and diagnostics.

Supporting Information

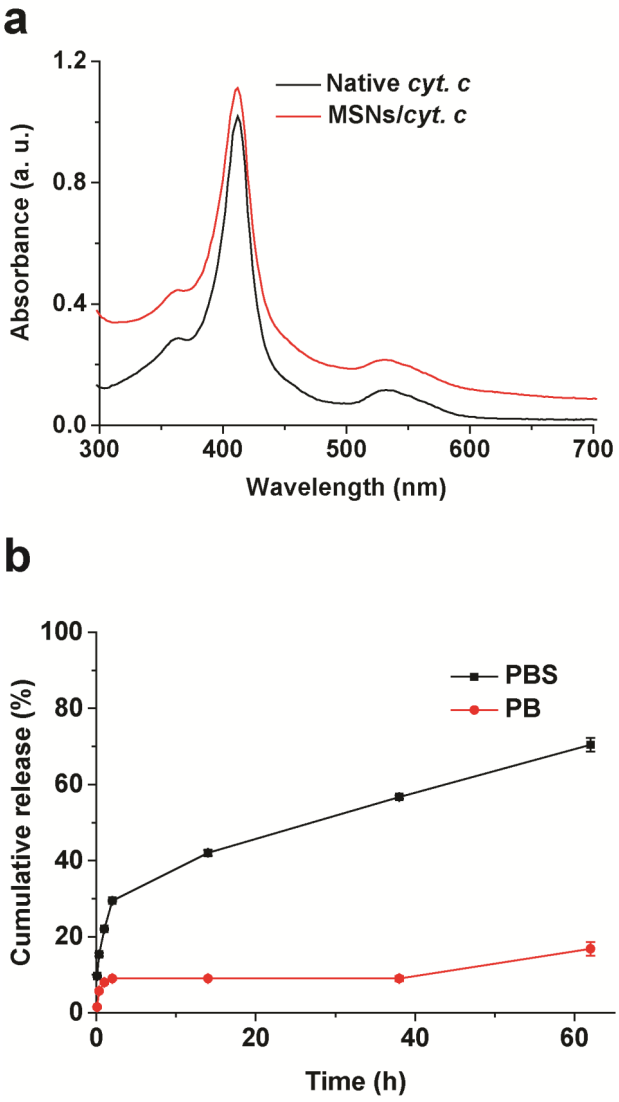

Figure 4.S1 *(a) UV-Visible adsorption spectra of free cyt. c and MSNs/cyt. c in 1 mM, pH 7.4. (b) Release profiles of MSNs/cyt. c in 1 mM PB and PBS, pH 7.4, 37 °C. Error bars show the standard deviation of three independent experiments.*

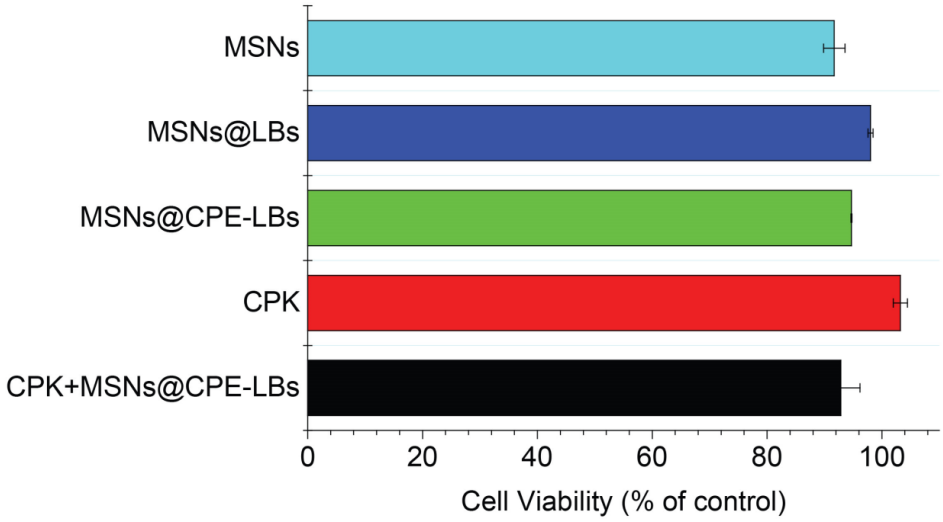

Figure 4.S2 *Cell viability by WST-1 of HeLa cells exposed to MSNs, MSNs@LBs with lipid composition of DOPC:DOPE:CHO (2:1:1), MSNs@CPE-LBs, CP_4K_4 and combinations thereof. Metabolic activity of untreated cells is 100%. Final concentrations: MSNs: 40 µg/ml, total lipids; 0.25 mM; CP_4K_4, CPE: 5 µM. Error bars show the standard deviation of three independent experiments.*

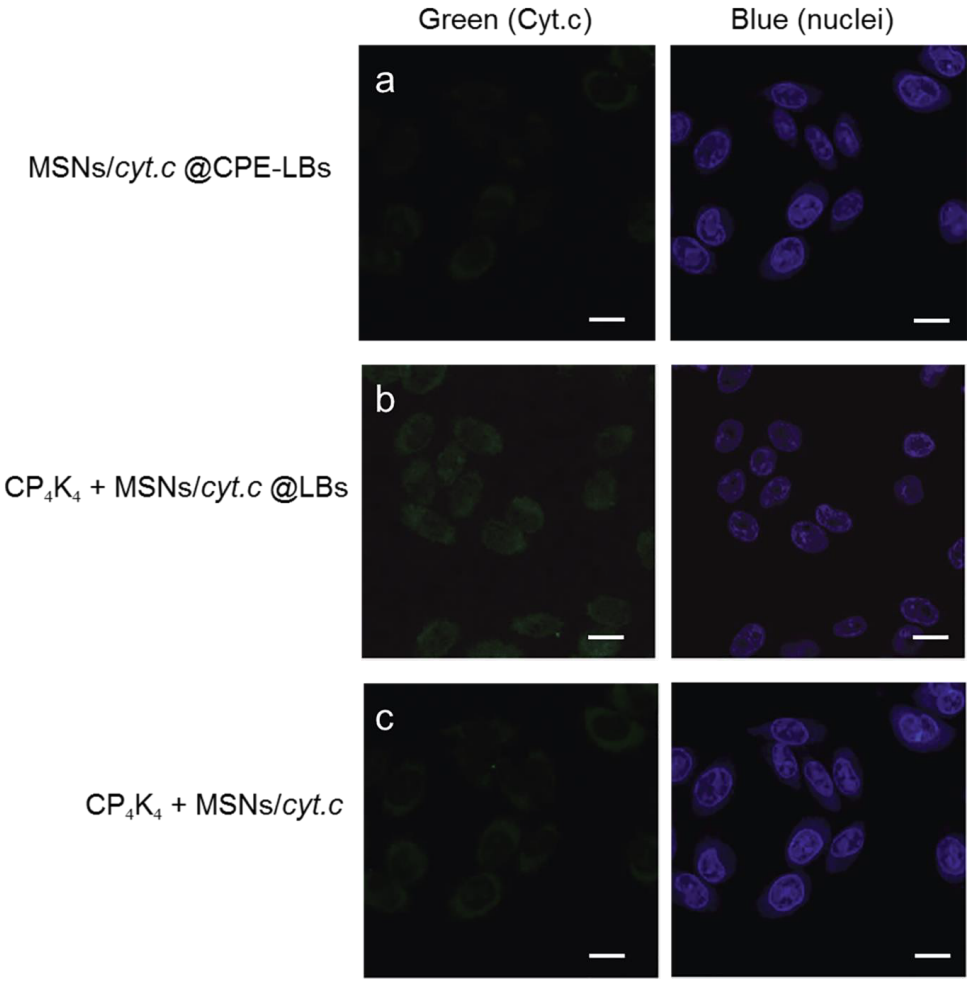

Figure 4.S3 *Delivery of cyt. c by MSNs@LBs is dependent on coiled-coil formation between CP_4K_4 and CP_4E_4. Confocal microscopy images of HeLa cells. Cells were pre-incubated with CP_4K_4 (b, c) or medium (a) for 2 h, followed by incubation with MSNs/cyt. c@LBs coated with peptide CPE (a) or no lipopeptide coating (b) and LBs coating (c) for 30 min. Images were taken after washing the cells several times with medium. Left panels: Atto 488 labeled cyt. c. Right panels: Hoechst staining. The final concentration of MSNs was 40 μg/ml. Scale bar = 25 μm.*

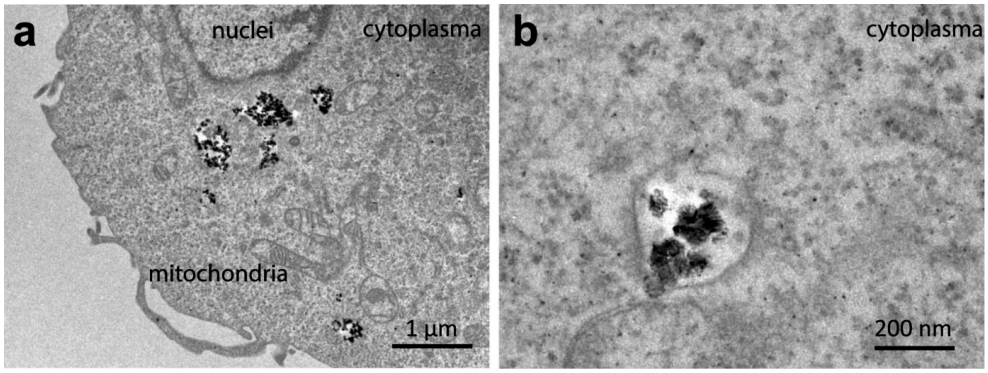

Figure 4.S4 *TEM images of HeLa cells. a) HeLa Cells were treated with bare MSNs for 0.5 h, after 3 times washing by medium, TEM images were taken. b) Magnification showing details of delivery, such as endosomal/lysosomal membrane.*

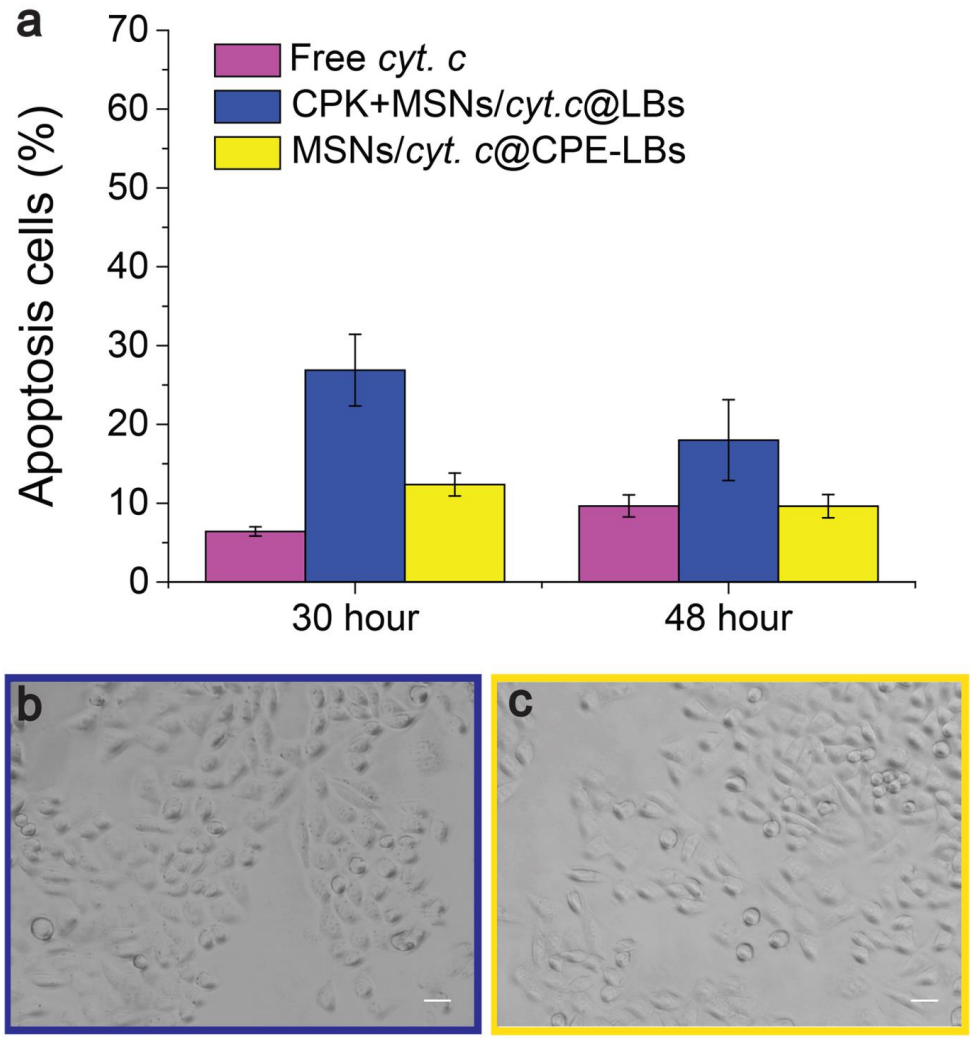

Figure 4.S5 *Apoptosis induced by MSNs/cyt. c@LBs in the absence of coiled-coil formation. a) HeLa cells were incubated with free cyt.c (purple bars), CP_4K_4 and MSNs/cyt.c @LBs (blue bars), or only MSNs/cyt. c@CPE-LBs (yellow bars). After several washing steps with medium apoptosis was assayed 30 h or 48 h later as described before. b) CP_4K_4 pre-treated cells incubated with MSNs/cyt.c@LBs. c) HeLa cells incubated with MSNs/cyt.c@CPE-LBs after 30 h treatment. Apoptotic cells are rarely seen in b and c. Error bars show the standard deviation of three independent experiments. Scale bar = 25 µm.*

4.5 References

1. Z. Gu, A. Biswas, M. Zhao and Y. Tang, *Chem. Soc. Rev.*, **2011**, 40, 3638-3655.
2. J. Ambati, A. M. Lopez, D. Cochran, P. Wattamwar, K. Bean, T. D. Dziubla and S. E. Rankin, *Acta Biomater.*, **2012**, 8, 2096-2103.
3. S. M. Kelly, T. J. Jess and N. C. Price, *Biochim. Biophys. Acta, Proteins Proteomics*, **2005**, 1751, 119-139.
4. F. P. Chang, Y. P. Chen and C. Y. Mou, *Small*, **2014**, 10, 4785-4795.
5. M. C. Manning, D. K. Chou, B. M. Murphy, R. W. Payne and D. S. Katayama, *Int. J. Pharm. Res.*, **2010**, 27, 544-575.
6. Y. Ikada and Y. Tabata, *Adv. Drug Delivery Rev.*, **1998**, 31, 287-301.
7. S. Lee, J. H. Ryu, K. Park, A. Lee, S. Y. Lee, I. C. Youn, C. H. Ahn, S. M. Yoon, S. J. Myung, D. H. Moon, X. Chen, K. Choi, I. C. Kwon and K. Kim, *Nano Lett.*, **2009**, 9, 4412-4416.
8. T. Vermonden, R. Censi and W. E. Hennink, *Chem. Rev.*, **2012**, 112, 2853-2888.
9. R. Censi, P. Di Martino, T. Vermonden and W. E. Hennink, *J. Controlled Release*, **2012**, 161, 680-692.
10. S. Martins, B. Sarmento, D. C. Ferreira and E. B. Souto, *Int. J. Nanomed.*, **2007**, 2, 595-607.
11. B. Chatin, M. Mevel, J. Devalliere, L. Dallet, T. Haudebourg, P. Peuziat, T. Colombani, M. Berchel, O. Lambert, A. Edelman and B. Pitard, *Mol. Ther.--Nucleic Acids*, **2015**, 4, e244.
12. E. Erikci, M. Gursel and I. Gursel, *Biomaterials*, **2011**, 32, 1715-1723.
13. S. P. Hudson, R. F. Padera, R. Langer and D. S. Kohane, *Biomaterials*, **2008**, 29, 4045-4055.
14. J. L. Vivero-Escoto, Slowing, II, B. G. Trewyn and V. S. Lin, *Small*, **2010**, 6, 1952-1967.
15. C. Argyo, V. Weiss, C. Bräuchle and T. Bein, *Chem. Mater.*, **2014**, 26, 435-451.
16. M. Y. Wu, Q. S. Meng, Y. Chen, L. X. Zhang, M. L. Li, X. J. Cai, Y. P. Li, P. C. Yu, L. L. Zhang and J. L. Shi, *Adv. Mater.*, **2016**, 28, 1963-1969.
17. T. L. Liu, H. Y. Liu, C. H. Fu, L. L. Li, D. Chen, Y. Q. Zhang and F. Q. Tang, *J. Colloid Interface Sci.*, **2013**, 400, 168-174.
18. J. Tu, T. X. Wang, W. Shi, G. S. Wu, X. H. Tian, Y. H. Wang, D. T. Ge and L. Ren, *Biomaterials*, **2012**, 33, 7903-7914.
19. S. Heidegger, D. Gossl, A. Schmidt, S. Niedermayer, C. Argyo, S. Endres, T. Bein and C. Bourquin, *Nanoscale*, **2016**, 8, 938-948.
20. S. H. van Rijt, D. A. Bölükbas, C. Argyo, S. Datz, M. Lindner, O. Eickelberg, M. Königshoff, T. Bein and S. Meiners, *ACS Nano*, **2015**, 9, 2377-2389.
21. C. E. Ashley, E. C. Carnes, G. K. Phillips, D. Padilla, P. N. Durfee, P. A. Brown, T. N. Hanna, J. Liu, B. Phillips, M. B. Carter, N. J. Carroll, X. Jiang, D. R. Dunphy, C. L. Willman, D. N. Petsev, D. G. Evans, A. N. Parikh, B. Chackerian, W. Wharton, D. S. Peabody and C. J. Brinker, *Nat. Mater.*, **2011**, 10, 389-397.
22. D. Mahony, A. S. Cavallaro, F. Stahr, T. J. Mahony, S. Z. Qiao and N. Mitter, *Small*, **2013**, 9, 3138-3146.
23. G. E. Francis, D. Fisher, C. Delgado, F. Malik, A. Gardiner and D. Neale, *Int. J. Hematol.*, **1998**, 68, 1-18.
24. A. Coscarella, R. Liddi, M. Di Loreto, S. Bach, A. Faiella, P. H. van der Meide, A. Mele and R. De Santis, *Cytokine*, **1998**, 10, 964-969.

25. E. C. Dengler, J. Liu, A. Kerwin, S. Torres, C. M. Olcott, B. N. Bowman, L. Armijo, K. Gentry, J. Wilkerson, J. Wallace, X. Jiang, E. C. Carnes, C. J. Brinker and E. D. Milligan, *J. Controlled Release*, **2013**, 168, 209-224.
26. J. G. Gribben, S. Devereux, N. S. Thomas, M. Keim, H. M. Jones, A. H. Goldstone and D. C. Linch, *Lancet*, **1990**, 335, 434-437.
27. V. Cauda, H. Engelke, A. Sauer, D. Arcizet, C. Brauchle, J. Radler and T. Bein, *Nano Lett.*, **2010**, 10, 2484-2492.
28. J. Zhang, D. Desai and J. M. Rosenholm, *Adv. Funct. Mater.*, **2014**, 24, 2352-2360.
29. R. A. Roggers, V. S. Lin and B. G. Trewyn, *Mol. Pharm.*, **2012**, 9, 2770-2777.
30. J. W. Liu, A. Stace-Naughton, X. M. Jiang and C. J. Brinker, *J. Am. Chem. Soc.*, **2009**, 131, 1354-1360.
31. H. Meng, M. Wang, H. Liu, X. Liu, A. Situ, B. Wu, Z. Ji, C. H. Chang and A. E. Nel, *ACS Nano*, **2015**, 9, 3540-3557.
32. B. A. Mora N, Valkenier H, Li H, Sharp T, Sheppard D, Davis A and Kros A, *Chem. Sci.*, **2016**, 7, 1768-1772.
33. H. Valkenier, N. Lopez Mora, A. Kros and A. P. Davis, *Angew. Chem., Int. Ed.*, **2015**, 54, 2137-2141.
34. F. Versluis, H. R. Marsden and A. Kros, *Chem. Soc. Rev.*, **2010**, 39, 3434-3444.
35. T. Zheng, J. Voskuhl, F. Versluis, H. R. Zope, I. Tomatsu, H. R. Marsden and A. Kros, *Chem. Commun.*, **2013**, 49, 3649-3651.
36. F. Versluis, J. Voskuhl, B. van Kolck, H. Zope, M. Bremmer, T. Albregtse and A. Kros, *J. Am. Chem. Soc.*, **2013**, 135, 8057-8062.
37. H. R. Marsden, N. A. Elbers, P. H. Bomans, N. A. Sommerdijk and A. Kros, *Angew. Chem., Int. Ed.*, **2009**, 48, 2330-2333.
38. H. R. Marsden, A. V. Korobko, T. Zheng, J. Voskuhl and A. Kros, *Biomater. Sci.*, **2013**, 1, 1046-1054.
39. H. R. Marsden, I. Tomatsu and A. Kros, *Chem. Soc. Rev.*, **2011**, 40, 1572-1585.
40. J. B. Yang, A.; Daudey, G.; Bussmann, J.; Olsthoorn, R.C.L.; Kros, A., *ACS Cent. Sci.*, **2016**, DOI: 10.1021/acscentsci.6b00172.
41. J. Yang, Y. Shimada, R. C. L. Olsthoorn, B. E. Snaar-Jagalska, H. P. Spaink and A. Kros, *ACS Nano*, **2016**, DOI: 10.1021/acsnano.6b01410.
42. J. C. Goldstein, C. Munoz-Pinedo, J. E. Ricci, S. R. Adams, A. Kelekar, M. Schuler, R. Y. Tsien and D. R. Green, *Cell Death Differ.*, **2005**, 12, 453-462.
43. E. P. H. Brunauer S. , Teller E., *J. Am. Chem. Soc.*, **1938**, 60, 11.
44. E. P. Barrett, L. G. Joyner and P. P. Halenda, *J. Am. Chem. Soc.*, **1951**, 73, 373-380.
45. Y. Han and J. Y. Ying, *Angew. Chem., Int. Ed.*, **2005**, 44, 288-292.
46. I. I. Slowing, B. G. Trewyn and V. S. Y. Lin, *J. Am. Chem. Soc.*, **2007**, 129, 8845-8849.
47. M. Ishiyama, M. Shiga, K. Sasamoto, M. Mizoguchi and P. G. He, *Chem. Pharm. Bull.*, **1993**, 41, 1118-1122.
48. E. S. Alnemri, D. J. Livingston, D. W. Nicholson, G. Salvesen, N. A. Thornberry, W. W. Wong and J. Yuan, *Cell*, **1996**, 87, 171.
49. B. L. Zhang, Z. Luo, J. J. Liu, X. W. Ding, J. H. Li and K. Y. Cai, *J. Controlled Release*, **2014**, 192, 192-201.
50. E. P. J. Barrett, L. E.; Halenda, P., *J. Am. Chem. Soc.*, **1951**, 73, 373-380.
51. X. Jiang and X. Wang, *Annu. Rev. Biochem.*, **2004**, 73, 87-106.
52. Y. Urabe, T. Shiomi, T. Itoh, A. Kawai, T. Tsunoda, F. Mizukami and K. Sakaguchi, *ChemBioChem*, **2007**, 8, 668-674.
53. C. H. Lee, J. Lang, C. W. Yen, P. C. Shih, T. S. Lin and C. Y. Mou, *J. Phys. Chem. B*, **2005**, 109, 12277-12286.

54. H. S. Park, C. Kim, H. J. Lee, J. H. Choi, S. G. Lee, Y. P. Yun, I. C. Kwon, S. J. Lee, S. Y. Jeong and S. C. Lee, *Nanotechnol.*, **2010**, 21, 225101.
55. J. Liu, X. Jiang, C. Ashley and C. J. Brinker, *J. Am. Chem. Soc.*, **2009**, 131, 7567-7569.
56. H. R. Zope, F. Versluis, A. Ordas, J. Voskuhl, H. P. Spaink and A. Kros, *Angew. Chem., Int. Ed.*, **2013**, 52, 14247-14251.
57. K. Epler, D. Padilla, G. Phillips, P. Crowder, R. Castillo, D. Wilkinson, B. Wilkinson, C. Burgard, R. Kalinich, J. Townson, B. Chackerian, C. Willman, D. Peabody, W. Wharton, C. J. Brinker, C. Ashley and E. Carnes, *Adv. Healthcare Mater.*, **2012**, 1, 348-353.
58. C. E. Ashley, E. C. Carnes, K. E. Epler, D. P. Padilla, G. K. Phillips, R. E. Castillo, D. C. Wilkinson, B. S. Wilkinson, C. A. Burgard, R. M. Kalinich, J. L. Townson, B. Chackerian, C. L. Willman, D. S. Peabody, W. Wharton and C. J. Brinker, *ACS Nano*, **2012**, 6, 2174-2188.
59. A. Arcaro and M. P. Wymann, *Biochem. J.*, **1993**, 296, 297-301.
60. N. Araki, M. T. Johnson and J. A. Swanson, *J. Cell Biol.*, **1996**, 135, 1249-1260.
61. C. K. Payne, S. A. Jones, C. Chen and X. Zhuang, *Traffic*, **2007**, 8, 389-401.
62. S. Coppola, L. C. Estrada, M. A. Digman, D. Pozzi, F. Cardarelli, E. Gratton and G. Caracciolo, *Soft Matter*, **2012**, 8, 7919-7927.
63. N. P. Gabrielson and D. W. Pack, *J. Controlled Release*, **2009**, 136, 54-61.
64. T. Akiyama, J. Ishida, S. Nakagawa, H. Ogawara, S. Watanabe, N. Itoh, M. Shibuya and Y. Fukami, *J. Biol. Chem.*, **1987**, 262, 5592-5595.
65. P. A. Orlandi and P. H. Fishman, *J. Cell Biol.*, **1998**, 141, 905-915.
66. L. H. Wang, K. G. Rothberg and R. G. Anderson, *J. Cell Biol.*, **1993**, 123, 1107-1117.
67. K. von Gersdorff, N. N. Sanders, R. Vandenbroucke, S. C. De Smedt, E. Wagner and M. Ogris, *Mol. Ther.*, **2006**, 14, 745-753.
68. U. S. Huth, R. Schubert and R. Peschka-Suss, *J. Controlled Release*, **2006**, 110, 490-504.
69. J. Rejman, V. Oberle, I. S. Zuhorn and D. Hoekstra, *Biochem. J.*, **2004**, 377, 159-169.
70. C. Goncalves, E. Mennesson, R. Fuchs, J. P. Gorvel, P. Midoux and C. Pichon, *Mol. Ther.*, **2004**, 10, 373-385.
71. S. Simoes, V. Slepushkin, N. Duzgunes and M. C. Pedroso de Lima, *Biochim. Biophys. Acta*, **2001**, 1515, 23-37.
72. H. Gao, Z. Yang, S. Zhang, S. Cao, S. Shen, Z. Pang and X. Jiang, *Sci. Rep.*, **2013**, 3, 2534.
73. X. Liu, C. N. Kim, J. Yang, R. Jemmerson and X. Wang, *Cell*, **1996**, 86, 147-157.
74. R. M. Kluck, E. Bossy-Wetzel, D. R. Green and D. D. Newmeyer, *Science*, **1997**, 275, 1132-1136.
75. Q. Chen, N. Takeyama, G. Brady, A. J. Watson and C. Dive, *Blood*, **1998**, 92, 4545-4553.
76. Q. Chen, B. Gong and A. Almasan, *Cell Death Differ.*, **2000**, 7, 227-233.